Magnetism of Fe films grown on Co(100) studied by spin-resolved Fe 3*s* photoemission

N. Kamakura,[1] A. Kimura,[2] T. Saitoh,[3] O. Rader,[4] K.-S. An,[5] and A. Kakizaki[6]
[1]*Soft X-ray Spectroscopy Laboratory, RIKEN/SPring-8, Sayo-cho, Sayo-gun, Hyogo 679-5148, Japan*
[2]*Department of Physical Science, Graduate School of Science, Hiroshima University, Higashi-Hiroshima, Hiroshima 739-8526, Japan*
[3]*Department of Applied Physics, Tokyo University of Science, Shinjuku-ku, Tokyo 162-8601, Japan*
[4]*Berliner Elektronenspeicherring-Gesellschaft für Synchrotronstrahlung (BESSY), Albert-Einstein-Strasse 15, D-12489 Berlin, Germany*
[5]*Thin Film Materials Laboratory, Korea Research Institute of Chemical Technology, Yuseong P.O. Box 107, Daejeon 305-600, Korea*
[6]*Institute for Solid State Physics (ISSP), The University of Tokyo, Kashiwanoha, Kashiwa, Chiba 277-8581, Japan*
(Received 15 June 2005; revised manuscript received 4 November 2005; published 24 March 2006)

The magnetic properties of fcc Fe films grown on fcc Co(100) have been studied by means of spin-resolved Fe 3*s* core-level photoemission and characteristics of the measured spin-resolved 3*s* spectra for fcc Fe films have been investigated. The spin-resolved 3*s* spectra measured on 3.9 and 6.6 monolayer (ML) fcc Fe films are similar in spectral shape. The 3*s* majority-spin spectra for these fcc Fe films show weaker intensity on the high-binding-energy side than the spectrum previously reported for bulk bcc Fe. The spin-resolved 3*s* spectra for the fcc Fe films are analyzed by cluster model calculation consisting of four Fe atoms. In the analysis by the cluster model calculation, effects of the interatomic configuration interaction on the spin-resolved 3*s* spectra for fcc Fe films are discussed. Itinerancy of 3*d* electrons is found to be an important factor in describing the spin-resolved Fe 3*s* spectra. The *z* spin momentum estimated by the cluster calculation indicates that both the Fe films are in a high-spin ferromagnetic state near the surface. On the other hand, the spin polarization at the background in the spectrum for the 6.6 ML Fe film is much smaller than that for the 3.9 ML film. This variation of the background spin polarization indicates that the magnetic moment averaged up to deeper layers of Fe film is suppressed in the 6.6 ML film.

DOI: 10.1103/PhysRevB.73.094437 PACS number(s): 75.70.Ak, 79.60.Dp

I. INTRODUCTION

The 3*d* transition metal thin films show a variety of magnetic properties depending on the film thickness, growth condition, and lattice misfit at the interface.[1–4] Ultrathin films with a few monolayers (ML) thickness exhibit quasi-two-dimensional magnetic properties such as the decrease of the Curie temperature (T_c) and the enhancement of the magnetic moment. Metastable structures that rarely stabilize in the bulk can appear in thin films grown pseudomorphically on appropriate substrates. In particular, fcc Fe thin films attract a lot of interest, since bulk Fe exhibits fcc structure only at high temperature between 1183 and 1663 K, which prevents full understanding of the magnetic properties of fcc Fe. Theoretically, the magnetic state of fcc Fe has been predicted to be quite sensitive to the lattice constant (a).[1,2,5–7] Total energy band calculations have shown that the nonmagnetic and antiferromagnetic states are energetically degenerate and most favorable for the lattice constant of ~3.5 Å, while the high-spin ferromagnetic state is stable for larger lattice constants ($a > 3.66$ Å).[1,2,5–7] Although the calculated results for the lattice constant (2.8 Å) and the magnetic moment ($2.12\mu_B$) of bcc Fe well reproduce the actual values of 2.87 Å and $2.22\mu_B$, respectively, the predicted properties of fcc Fe have not been fully examined in bulk and the complicated magnetic states of fcc Fe have been studied using Fe thin films grown on Cu,[8–15] $Cu_{1-x}Au_x$,[16] fcc Co,[17–23] and Rh (Ref. 24) substrates.

Iron thin films grown on fcc Co(100) exhibit the fcc structure below 11 ML and transform into the bcc structure at 11 ML (region III).[17–23] The structure below 11 ML is distinguished further into two regions (regions I and II) at 5 ML by the difference in the layer distance. In the thin film of region I with the film thickness below 5 ML, the fcc structure is tetragonally distorted. The tetragonal distortion is relaxed and an almost isotropic fcc structure is stabilized except for the expanded two topmost layers in region II with the film thickness between 5 and 10 ML. This difference in the layer distance affects the magnetism of the Fe thin film, as expected by the total energy band calculation,[1,2,5–7] and causes the following thickness-dependent magnetic properties which have been supported by the several experiments.[17–23] The whole Fe thin film in region I is in a ferromagnetically ordered high-spin state, while the ferromagnetic order in the Fe thin film of region II is restricted to the two topmost layers and the two layers at the interface. The ferromagnetic order at the interface is induced by the ferromagnetic Co substrate.[17,22] The inner layers of the Fe thin film in region II have been believed to be paramagnetic or antiferromagnetic. A previous x-ray magnetic circular dichroism (XMCD) study[23] has suggested antiferromagnetic order in inner layers of region II films, whereas the detailed magnetic structure in these layers has not been determined.

In this work, we have performed Fe 3*s* spin-resolved photoemission spectroscopy (SRPES) to study the spin-dependent electronic states of Fe/Co(100). The 3*s* photoemission spectroscopy of 3*d* transition metals has been extensively studied in terms of its applicability to estimation of the local spin moment.[25–38] The exchange splitting into high-spin (HS) ($S+1/2$) and low-spin (LS) ($S-1/2$) final

states (where S represents the total spin in an atom) in the 3s photoemission spectrum is caused by the exchange interaction between the total spin in the valence band and core-level spin left in the final state. According to the Van Vleck theorem,[25] the energy separation of these two final states is expressed as $J(S+1/2)$, which includes the total spin. The intensity ratio between the majority- and minority-spin spectra in the HS state, $I_{HS\uparrow}/I_{HS\downarrow}$, which determines the spin polarization in the HS state, also reflects the spin moment and is given by $2S+1$.[39] However, the atomic model described above has sometimes shown inconsistencies in the estimation of the local spin moment.[27] Therefore, we have analyzed the experimental Fe 3s SRPES spectra by a cluster model consisting of four atoms to quantitatively estimate parameters such as z spin momentum and have discussed the characteristics of the Fe 3s SRPES spectra of fcc Fe/Co(100).

II. EXPERIMENT

The SRPES measurements were carried out at undulator beamline[40] BL-19A of the Photon Factory, which is equipped with a hemispherical electron energy analyzer and a 100 keV Mott detector[41] for spin analysis. For the preparation of Fe/Co(100), the fcc Co(100) thin film was prepared on a Cu(100) clean surface, followed by Fe growth on the obtained fcc Co(100) thin film. The Cu(100) clean surface was checked by Auger electron spectroscopy (AES) and the surface crystallinity was confirmed by low-energy electron diffraction. The Co and Fe thin films were evaporated at room temperature (RT) by electron bombardment of high-purity metal wires. The layer-by-layer growth was confirmed by the oscillation of the reflection intensity of high-energy electron diffraction. The nonexistence of interdiffusion and cleanliness of the thin films were checked by AES before and after every SRPES measurement.

The obtained Fe thin films were remanently magnetized by applying a magnetic field along the [110] direction, which is parallel to the surface. We confirmed that the spin polarization of inelastically scattered electrons, which was measured at some energy points with higher accuracy, was saturated by this magnetic field. A previous XMCD study on Fe/Co(100) has shown that the coercive fields for Fe and Co are identical.[17] In Ref. 17, the hysteresis loops for Fe on Co(100) did not show large differences between the remanent magnetizations and saturation magnetizations. The SRPES measurements on 3.9 and 6.6 ML Fe/Co(100) were performed at RT and 130 K, respectively. The previous study of Fe/Co(100) by the magnetic dichroism in the Fe 2p photoemission spectrum using Mg $K\alpha$ x radiation indicated that the difference between the dichroism spectra at 200 K and RT was negligible in region II.[21] The spin polarization of inelastically scattered electrons was essentially unchanged during the SRPES measurements. The spectra were measured using $h\nu=167$ eV at normal emission and the energy resolution was set to 200 meV. The Co 3s signal was already negligible in the 3s spectrum of 3.9 ML Fe/Co(100), which was also confirmed by the 3p spectrum.

III. RESULTS AND DISCUSSION

Figures 1(a) and 1(b) show the Fe 3s SRPES spectra of 3.9 and 6.6 ML Fe films, as representatives of the region I and II films, respectively. In each of Figs. 1(a) and 1(b), the minority-spin spectrum shows a clear peak [A in Fig. 1(a) and A' in Fig. 1(b)] corresponding to the HS state and the majority-spin spectrum shows a weaker peak, which is attributable to the majority-spin component of the HS state, at the binding energy near the peak in the minority-spin spectrum. In addition, there is an additional spectral weight on the high-binding-energy side of these peaks in each majority-spin spectrum of Figs. 1(a) and 1(b). This spectral weight may be attributed to the LS state, whereas its intensity is weaker than the LS state observed in the 3s majority-spin spectrum for bcc Fe.[31–37] The spin polarizations corresponding to the SRPES spectra in Figs. 1(a) and 1(b) are shown in Figs. 1(c) and 1(d), respectively. The spin polarizations in the HS states marked with A and A' for 3.9 and 6.6 ML Fe, respectively, show the comparable reductions ($\sim$10%) from the background spin polarizations [Figs. 1(c) and 1(d)]. It indicates that the magnetic moments in regions I and II are essentially equal near the surface. However, the spin polarizations of inelastically scattered electrons show a marked difference. The spin polarization averaged between 105.0 and 110.0 eV binding energies is estimated to be (20.6±0.3)% in 3.9 ML Fe [Fig. 1(c)], and is drastically reduced to (11.5±0.3)% in 6.6 ML Fe [Fig. 1(d)]. This clear change of the background spin polarization shows that the magnetic moment integrated over the probing depth of inelastically scattered electrons forming the background is suppressed in region II. The background spin polarization of 2.3

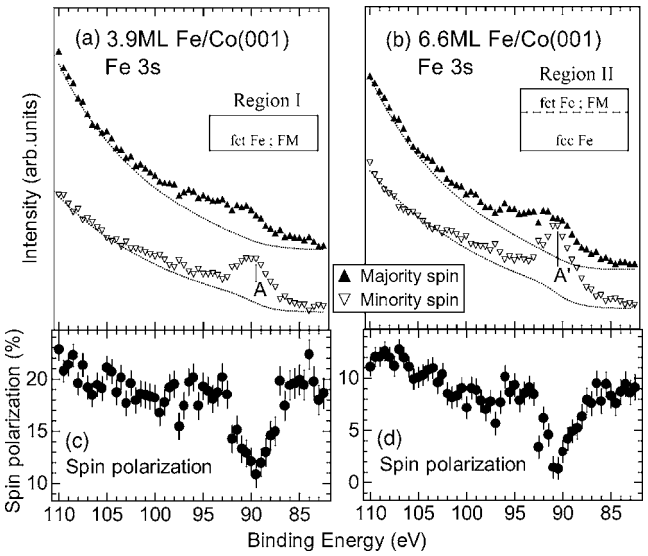

FIG. 1. The raw Fe 3s SRPES spectra for (a) 3.9 and (b) 6.6 ML Fe on Co(100). Upward and downward triangles show the majority- and minority-spin spectra, respectively. The Shirley backgrounds are also indicated by the dotted lines. The peak in the minority-spin spectrum for 3.9 (6.6) ML Fe is marked with $A(A')$. The insets in (a) and (b) show the structures and ferromagnetic (FM) layers in the corresponding thickness regions. The fct in the insets indicates the tetragonally distorted fcc structure. In region II, the ferromagnetic order exists also in the two layers at the interface as well as the two topmost layers shown in the inset of (b). (c) and (d) show the spin polarizations corresponding to the SRPES spectra in (a) and (b), respectively.

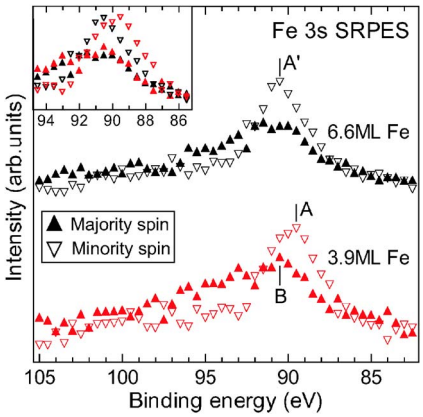

FIG. 2. (Color online) The Fe 3*s* SRPES spectra for 3.9 and 6.6 ML Fe on Co(100), in which the Shirley backgrounds are subtracted from the raw spectra. Upward and downward triangles show the majority- and minority-spin spectra, respectively. The peak in the minority-spin spectrum for 3.9 (6.6) ML Fe is marked with $A(A')$ and the peak in the majority-spin spectrum for 3.9 ML Fe is marked with *B*. The SRPES spectra of the two Fe thin films are superimposed in the inset. The SRPES spectra for 3.9 and 6.6 ML Fe are shown by red and black triangles, respectively.

ML Fe, which has been also measured at RT, is $(20.4\pm0.3)\%$. Since this value is equal to the background spin polarization of 3.9 ML Fe within the error bars and substantially different from that of 6.6 ML Fe, the background spin polarization can be regarded as probing the difference between the magnetic moments of Fe thin films in regions I and II. These results indicate that the magnetic moment of deeper Fe layers is suppressed in region II.

Since the raw Fe 3*s* SRPES spectra shown in Fig. 1 include the background of inelastically scattered electrons, we have estimated Shirley backgrounds for the individual SRPES spectra, as indicated in Fig. 1. The Fe 3*s* SRPES spectra after the subtractions of these backgrounds are shown in Fig. 2. In Fig. 2, the sharp peak A (A') is observed at about 89.5 (90.5) eV in the minority-spin spectrum of 3.9 (6.6) ML Fe. The spectral shapes of the majority-spin spectra are broad. The main peak *B* in the majority-spin spectrum of 3.9 ML Fe, which can correspond to the HS state in the atomic model, is located at about 90.5 eV. In the Fe 3*s* SRPES spectrum of bulk bcc Fe reported in Ref. 35, a clear two-peak structure has been observed in the majority-spin spectrum. These two peaks can be attributed to the LS and HS states, which were separated by 3.5 eV, and the ratio of the two peaks was estimated to be 1.72:1. The minority-spin spectrum of bcc Fe shows a single peak corresponding to the HS state. The two components, majority and minority spin, of the HS state were separated by 0.9 eV. The 3*s* SRPES spectrum for 3.9 ML Fe shown in Fig. 2 appears to also indicate an energy separation between the HS states in majority- and minority-spin spectra, whereas the majority-spin spectrum for 6.6 ML Fe shows the peak located at the energy position of peak A'. This can also be found from the inset of Fig. 2, in which peak A in the minority-spin spectrum of 3.9 ML Fe evidently shifts to lower binding energy than peak A' in that of 6.6 ML Fe. It shows that, with respect to the peak in the minority-spin spectrum, the peak in the majority-spin spectrum is located at higher binding energy for 3.9 ML Fe than for 6.6 ML Fe, which further supports the energy separation between the HS states in the majority- and minority-spin spectra of 3.9 ML Fe. This is not due to the background subtraction, because also in the raw SRPES spectrum of 3.9 ML Fe shown in Fig. 1(a) the peak in the majority-spin spectrum is located at slightly higher binding energy than the peak in the minority-spin spectrum (peak *A*), while these peak positions overlap in Fig. 1(b). The difference between the raw Fe 3*s* SRPES spectra of 3.9 and 6.6 ML Fe is found in the spin polarization [Figs. 1(c) and 1(d)]. The minimum of the spin polarization is located at 89.5 eV in Fig. 1(c), while the minimum shifts to 90.5 eV in Fig. 1(d). This energy shift reflects the energy difference between peaks A and A'. The peak in the raw majority-spin spectrum of 3.9 ML Fe is located at slightly higher binding energy than the minimum of the spin polarization. These characteristics indicate that the HS state in the majority-spin spectrum of 3.9 ML Fe is located at higher binding energy than the HS state in the minority-spin spectrum, whereas these positions overlap in the SRPES spectrum of 6.6 ML Fe. Also after background subtraction, the spectral intensity on the high-binding-energy side (~93–97 eV) in each majority-spin spectrum for 3.9 and 6.6 ML Fe is weaker than the intensity of the LS state in the Fe 3*s* majority-spin spectrum reported for bulk bcc Fe.[31–37]

To analyze the spectral profile of the Fe 3*s* SRPES spectra, we have adopted a cluster model calculation which consists of four atoms.[31] This model takes account of the interatomic configuration interaction by describing the bases in the electron occupancies of the four atomic sites and considering the electron hopping between the neighboring sites to give a better picture for the 3*s* SRPES spectrum in 3*d* transition metals of itinerant electron systems. The model Hamiltonian H based on the Hubbard model consists of the two parts H_d and H_c, which represent the interaction among 3*d* electrons and the interaction between the 3*s* and 3*d* electrons, respectively, as

$$H = H_d + H_c,$$

$$H_d = \sum_{\langle i,j \rangle} t_{ij} \hat{\Psi}_i^\dagger \hat{\Psi}_j + U \sum_{i,\mu,\nu} n_{i,\mu} n_{i,\nu},$$

$$H_c = -Q \sum_{\sigma,\mu} (1 - n_{c,\sigma}) n_\mu - J(SS_c) + \varepsilon_c \sum_\sigma \hat{\Psi}_{c,\sigma}^\dagger \hat{\Psi}_{c,\sigma}. \quad (1)$$

H_d includes the 3*d*-3*d* on-site Coulomb interaction U and the hopping integral t_{ij} between the nearest-neighbor i and j sites. H_c consists of the Coulomb interaction Q and exchange interaction J between the 3*s* and 3*d* electrons on the site. A basis describing the ground state is specified by the number of 3*d* electrons $(n_{d,\sigma})$ occupying each site with spin σ as

$$|\phi_p\rangle = |(n_{d,\uparrow})_1, (n_{d,\downarrow})_1\rangle |(n_{d,\uparrow})_2, (n_{d,\downarrow})_2\rangle |(n_{d,\uparrow})_3, (n_{d,\downarrow})_3\rangle \times |(n_{d,\uparrow})_4, (n_{d,\downarrow})_4\rangle. \quad (2)$$

The averaged z spin momentum $\langle S_z \rangle$ and averaged 3*d* electron number $\langle n_d \rangle$ in the four-atom cluster, which are intro-

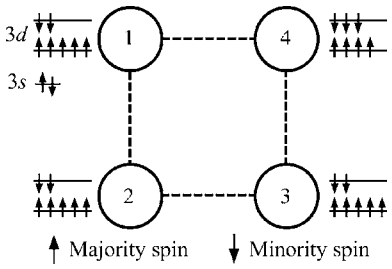

FIG. 3. The configuration $(5,5,5,4)_{\uparrow},(2,2,2,3)_{\downarrow}$ in the four-atom cluster model.

duced as parameters, govern the electron occupancies of the majority- and minority-spin states at the four sites and are assumed to be conserved through the calculation. Thus, this model takes short-range magnetic order into account. For the example of $\langle S_z\rangle=1.25$ and $\langle n_d\rangle=7.0$, one of the possible configurations is written as $(5,5,5,4)_{\uparrow}$, $(2,2,2,3)_{\downarrow}$ (Fig. 3), in which $(n_1,n_2,n_3,n_4)_{\sigma}$ represents the number of $3d$ electrons at individual sites with spin σ. The ground state, which is represented by the linear combination of the basis (2) satisfying $\langle S_z\rangle$ and $\langle n_d\rangle$ given as parameters, is obtained by the modified Lanczos method using H_d.[42] For description of the final state, a core hole is introduced in the $3s$ state at one site of the cluster, which is fixed at the site 1. Thus, not every site is equivalent in the final state because of the presence of the core hole in site 1. The basis describing the final state is written as

$$|\phi_p^f\rangle=\hat{a}_{3s}|\phi_p\rangle=|(n_{d,\uparrow})_1,(n_{d,\downarrow})_1,s_z^c\rangle|(n_{d,\uparrow})_2,(n_{d,\downarrow})_2\rangle \times|(n_{d,\uparrow})_3,(n_{d,\downarrow})_3\rangle|(n_{d,\uparrow})_4,(n_{d,\downarrow})_4\rangle, \quad (3)$$

where s_z^c is the z momentum of the $3s$ core-level spin at site 1. The spectral function is obtained from the Green function, which is calculated by the Haydock recusion method using H.[43] This calculation has been started from the state in which the $3s$ core hole is added to the above obtained initial state and continued until the calculated result converges.

In Figs. 4(a) and 4(b), the calculated results for the Fe $3s$ SRPES spectra of 3.9 and 6.6 ML Fe/Co(100) by the four-atom cluster model are overlaid with the experimental spectra. The parameters estimated by the calculation are listed in Table I. The calculation well reproduces the characteristics of the experimental $3s$ SRPES spectrum for 3.9 ML Fe, such as the weak intensity (C) on the high-binding-energy side in the majority-spin spectrum and the intensity ratio between peaks A and B. The discrepancy between the measured spectrum and cluster calculation still remains in the spectral weight near the main peak in the majority-spin spectrum for 6.6 ML Fe, which will be discussed later. The experimental minority-spin spectra for both the Fe thin films are well fitted by the calculated curves. The peaks in the calculated minority-spin spectra of 3.9 and 6.6 ML Fe are located at 89.7 and 90.5 eV, respectively. Thus, the energy difference between peaks A and A', which is depicted in the inset of Fig. 2, is estimated to be about 0.8 eV. We have performed a lot of calculations to describe the Fe $3s$ SRPES spectra of fcc Fe thin films. In the calculation, we have specified the parameters $\langle S_z\rangle$ and

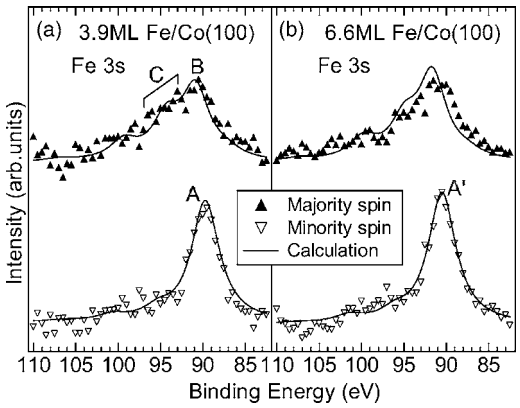

FIG. 4. The Fe $3s$ SRPES spectra for (a) 3.9 and (b) 6.6 ML Fe on Co(100), shown in Fig. 2, are compared to the calculated spectra. Upward and downward triangles indicate the observed majority- and minority-spin spectra. The solid lines in (a) and (b) show the Fe $3s$ SRPES spectra calculated using the parameters listed in Table I. The peak in the minority-spin spectrum for 3.9 (6.6) ML Fe is marked with $A(A')$ and the peak in the majority-spin spectrum for 3.9 ML Fe is marked with B. In the majority-spin spectrum for 3.9 ML Fe, the spectral structure on the high-binding-energy side of peak B is denoted by C.

$\langle n_d\rangle$ first. In both 3.9 and 6.6 ML Fe thin films, the best results are obtained from $\langle n_d\rangle=7.5$ and $\langle S_z\rangle=1.0$. The magnetic moments in regions I and II are therefore equal near the surface, which is consistent with the result shown by the spin polarization. $\langle S_z\rangle=1.0$ corresponds to the magnetic moment of $2.0\mu_B$, which is consistent with the value predicted for the high-spin ferromagnetic state of fcc Fe by a total energy band calculation.[1,2,5–7] This result is also consistent with the previous experimental studies showing the high-spin ferromagnetic state for the Fe thin film on Co(100) in region I.[18–20,22] The detailed magnetic state of the ferromagnetic layers near the surface in region II has not been discussed so far. Our result shows that the magnetic moment near the surface in region II is equivalent to that in region I and both the Fe films are in the high-spin ferromagnetic state near the surface. Although the band structure calculation has indicated the total valence electron number of 7.244 for the high-spin ferromagnetic state of fcc Fe (Ref. 7), in the present study the calculation using $\langle n_d\rangle=7.5$ finally leads to better fitting results than that using $\langle n_d\rangle=7.25$. The larger value of $\langle n_d\rangle$ in our estimation can be derived from core-hole screening in the final state from outside of the model cluster.

TABLE I. The parameters estimated for 3.9 and 6.6 ML Fe from the four-atom cluster model analyses of the Fe $3s$ SRPES spectra. The parameters for bulk bcc Fe (Ref. 31) are also listed. (t, J, U, Q in units of eV.)

Sample	$\langle S_z\rangle$	t	J	U	Q
3.9 ML Fe	1.0	2.2	2.5	2.2	2.0
6.6 ML Fe	1.0	2.5	2.3	1.8	1.8
bcc Fe[a]	1.25	1.1	3.1	3.5	3.5

[a]Reference 31.

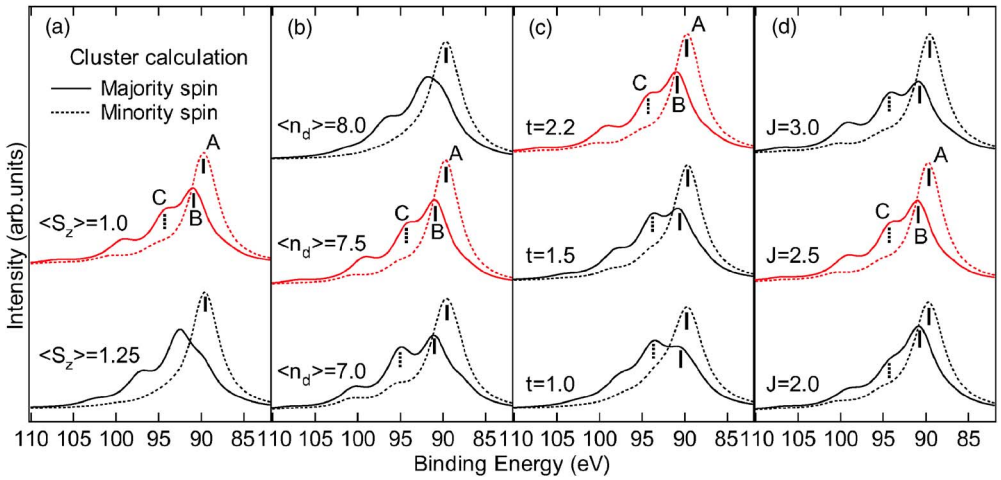

FIG. 5. (Color online) The dependences of the 3*s* SRPES spectrum on the parameters $\langle S_z \rangle$, $\langle n_d \rangle$, t, and J are examined by the calculation using the four-atom cluster model. The parameters except for (a) $\langle S_z \rangle$, (b) $\langle n_d \rangle$, (c) t, or (d) J are fixed at the values in the calculation for 3.9 ML Fe. The calculated majority- and minority-spin spectra are shown by the solid and broken lines, respectively. The red curves indicate the 3*s* SRPES spectrum calculated from the parameters for 3.9 ML Fe. *A* and *B* with bars denote the peaks in the majority- and minority-spin spectra calculated from the parameters for 3.9 ML Fe, respectively. *C* with dotted bar represents the spectral structure on the high-binding-energy side of peak *B* in the majority-spin spectrum calculated from the parameters for 3.9 ML Fe. Also in the spectra except for the calculated spectrum of 3.9 ML Fe shown by the red curves, the peaks corresponding to *A* and *B* are marked with bars, and the peaks corresponding to *C* are marked with dotted bars.

Since the values of $\langle S_z \rangle$ and $\langle n_d \rangle$ are discretely changed in our cluster model consisting of four atoms, their variations cause discontinuous changes of the spectral shape. Figure 5(a) shows a calculation in which only the $\langle S_z \rangle$ is changed from 1.0 to 1.25 and the other parameters are fixed at the values in the calculation for 3.9 ML Fe. In the majority-spin spectrum calculated using $\langle S_z \rangle = 1.25$, the main peak is located at about 93 eV and a shoulder is present at about 90 eV, which is equal to the peak position of the minority-spin spectrum. These features correspond to the LS and HS states in the atomic model, whereas the calculation shows an additional structure at about 97 eV in the majority-spin spectrum obtained by considering electron hopping. The calculation using $\langle S_z \rangle = 1.25$ is not consistent with the experimental 3*s* SRPES spectra for the fcc Fe thin films in the main peak position of the majority-spin spectrum. In the SRPES spectrum calculated using $\langle S_z \rangle = 1.00$, which is identical with the calculated spectrum for 3.9 ML Fe, the spectral weight of the shoulder at about 90 eV in the majority-spin spectrum disappears and, instead, the main peak in the majority-spin spectrum (peak *B*) appears at slightly higher binding energy than the peak in the minority-spin spectrum (peak *A*). There is a weak structure (peak *C*) at higher binding energy than peak *B*. These features are not predicted by the atomic model, but are consistent with the 3*s* SRPES spectrum of 3.9 ML Fe. For $\langle S_z \rangle = 1.25$ with $\langle n_d \rangle = 7.5$, the configurations with electron distributions such as $(5,5,5,5)_\uparrow$, $(2,2,3,3)_\downarrow$ [Fig. 6(a)] bring the Coulomb energy among the 3*d* electrons in the cluster to the minimum, because these configurations correspond to the most homogeneous electron distribution for the given $\langle S_z \rangle$ and $\langle n_d \rangle$, and minimize the Coulomb energy in the cluster, that is, the summation of the on-site Coulomb interaction U in the four sites. Hence, these configurations are expected to be weighted by the largest amplitude in the ground state. In these configurations, however, the majority-spin electrons cannot move to other sites. On the other hand, the minimum of the Coulomb energy is obtained by the configurations with electron distributions such as $(5,5,5,4)_\uparrow$, $(2,2,3,4)_\downarrow$, and $(5,5,5,4)_\uparrow$, $(2,3,3,3)_\downarrow$ [Fig. 6(b)] for $\langle S_z \rangle = 1.00$ with $\langle n_d \rangle = 7.5$. The majority-spin electrons can move to other sites in these configurations and the calculated spectrum shows features that are not predicted by the atomic model. Thus, the change of $\langle S_z \rangle$ influences the majority-spin spectrum through the spin arrangement at each site, which governs the degree of interatomic configuration interaction. Hence, the interatomic configuration interaction affects 3*s* SRPES spectra.

The number of the occupied 3*d* electrons $\langle n_d \rangle$ is estimated to be 7.5 in the calculation of Fig. 4. The dependence of the calculated 3*s* SRPES spectrum on the electron occupation is shown in Fig. 5(b), where the parameters except for $\langle n_d \rangle$ are fixed at the values for 3.9 ML Fe. In the majority-spin spectrum of $\langle n_d \rangle = 8.0$, the main peak is located at about 92 eV and there is a shoulder at about 2 eV lower binding energy than the main peak. The energy position of the shoulder is

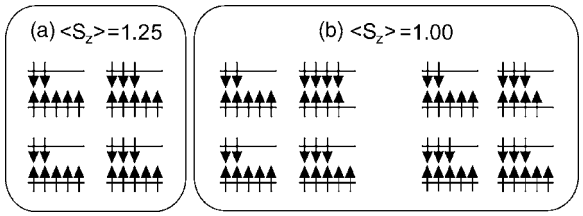

FIG. 6. The configurations (a) $(5,5,5,5)_\uparrow$,$(2,2,3,3)_\downarrow$ and (b) $(5,5,5,4)_\uparrow$,$(2,2,3,4)_\downarrow$ and $(5,5,5,4)_\uparrow$,$(2,3,3,3)_\downarrow$. The configurations shown in (a) and (b) bring the Coulomb energy among the 3*d* electrons to the minimum for $\langle S_z \rangle = 1.25$ and 1.00 with $\langle n_d \rangle = 7.5$, respectively.

approximately equal to the main peak of the minority-spin spectrum. As in the spectrum with $\langle S_z \rangle = 1.25$ shown in Fig. 5(a), these features are reminiscent of the LS and HS states described by the atomic model, whereas the calculation with $\langle n_d \rangle = 8.0$ is not consistent with the experimental majority-spin spectrum in the main peak position. The change of the spectral shape with decreasing $\langle n_d \rangle$ is somewhat similar to the change with the variation of $\langle S_z \rangle$ from 1.25 to 1.00. With the decrease in $\langle n_d \rangle$, thus, deviation from the atomic model becomes obvious. This tendency is also associated with more effective interatomic configuration interaction caused by electron hopping with lower occupation. At $\langle n_d \rangle = 7.0$, peak *C* shifts to higher binding energy and its relative intensity increases. The relative intensity of peak *C* in the spectrum calculated from $\langle n_d \rangle = 7.0$ is too large compared to that in the experimental majority-spin spectrum.

As a result of these calculations varying $\langle S_z \rangle$ and $\langle n_d \rangle$, the parameters $\langle S_z \rangle = 1.0$ and $\langle n_d \rangle = 7.5$ are determined. After fixing $\langle S_z \rangle$ and $\langle n_d \rangle$, we have optimized the other parameters. If the parameters estimated for the fcc Fe thin films are compared to those of bcc Fe, which are reported in Ref. 31 and also listed in Table I, it is found that *t* in 3.9 ML fcc Fe thin film is twice as large as that obtained in bcc Fe. Therefore, we examine the dependence of the spectral shape on *t* to confirm the validity of the parameter *t*. Figure 5(c) is the calculated 3*s* spectrum, in which only *t* is decreased from the value (2.2 eV) for 3.9 ML Fe. With the decrease in *t* from 2.2 eV, the intensity of peak *B* relative to peak *A* and peak *C* decreases and the inconsistency between the measured spectrum and calculation becomes evident in the relative intensities of peaks *B* and *C*. The SRPES spectrum with small *t* ($t = 1.0$ eV) develops a feature corresponding to the HS and LS states expected by the atomic model. Thus, our calculation for fcc Fe thin films results in much larger *t* than that estimated for bcc Fe. The spectral change with increasing *t* is similar to the change with decrease in $\langle n_d \rangle$ and with the variation of $\langle S_z \rangle$ from 1.25 to 1.0, while the change with the variation in *t* is properly continuous. This similarity indicates that the variation of $\langle S_z \rangle$ from 1.25 to 1.0 and the decrease in $\langle n_d \rangle$ indeed bring a more effective interatomic configuration interaction by electron hopping between the nearest-neighbor sites.

In Fig. 5(d), the dependence of the spectral shape on *J* is also examined by the calculation, because the Van Vleck theorem expects that the exchange splitting in the 3*s* spectrum is proportional to *J*. In our calculation considering electron hopping with relatively large *t* ($t = 2.2$ eV), however, the variation in *J* affects the relative intensities of peaks *B* and *C* rather than the energy positions of the individual peaks. As shown in Fig. 5(d), with increasing *J*, the intensity of peak *B* relative to peaks *A* and *C* is reduced, and hence the relative intensity of peak *C* increases. This feature is consistent with the result indicated in Ref. 31, which reported the analysis of spin-integrated 3*s* spectrum by the four-atom cluster model. The calculation using $J = 2.5$ provides better fitting result for the SRPES spectrum of 3.9 ML Fe than that using $J = 3.0$, which is close to the value estimated for bcc Fe in Ref. 31, and results in the most appropriate intensities of peaks *B* and *C* for reproducing the experimental spectrum of 3.9 ML Fe. The values of the parameters *U* and *Q* have also been determined so that the calculation provides the best fitting result. Although the dependence of the spectral shape on each parameter involves some similar features, it also shows behavior peculiar to each parameter, in terms of the relative intensities of the spectral structures and their relative energy positions. The parameters in Table I have been finally determined so that the calculation reproduces the characteristics of the experimental spectra, such as the intensity ratio between peaks *B* and *A*, the intensity on the high-binding-energy side of peak *B* in the majority-spin spectrum, and the energy position of peak *B*. Our calculation shows that *t* in the fcc Fe thin film is much larger than that in bcc Fe.[31] Since the experimental majority-spin spectra of the fcc Fe thin films actually show weaker intensity on the high-binding-energy side of peak *B* than that of bulk bcc Fe, the difference in the parameters would reflect the difference of the lattice structure. The majority-spin spectrum calculated from larger *t* results in the lower intensity of the high-binding-energy structure. Thus, the difference between the 3*s* spectra of the fcc thin film and bcc Fe is attributable mainly to the interatomic parameter *t*.

To elucidate the difference between the *t* values in the fcc Fe thin film and bcc Fe qualitatively, we compare the locations and numbers of neighboring atoms. The distance to nearest-neighbor atoms in the fcc Fe thin film, which is expected to be equivalent to that in the substrate fcc Co (~ 2.55 Å) (Ref. 44) in plane, is slightly longer than that in bcc Fe (~ 2.48 Å). However, the number of nearest neighbors is eight in the bcc structure and 12 in the fcc structure. Although, in a real Fe thin film on Co(100), the fcc structure is tetragonally distorted for the whole Fe film in region I and the two topmost layers in region II, the distance to the distorted eight sites is still close to the distance to the nearest-neighbor sites in plane.[45] Thus, the 3*d* orbital in the Fe thin films will show more itinerant character than that in bulk bcc Fe. Since the electron hopping in these structures is described by the electron hopping between the two nearest-neighbor sites within the cluster in the framework of our model, the calculations by the four-atom cluster model provide larger values of *t* for 3.9 and 6.6 ML Fe thin films than for bcc Fe. Larger *t*, i.e., a more delocalized 3*d* state, leads to smaller *J* as listed in Table I because of weaker overlap between the wave functions of 3*s* and 3*d* orbitals. Smaller *J* also contributes to the feature in the 3*s* majority-spin spectra of the fcc Fe thin films, showing the weaker intensity on the high-binding-energy side. The smaller values of *Q* and *U* in the fcc Fe thin films are also expected due to the more delocalized 3*d* orbital, since Coulomb interaction tends to become larger for more localized orbitals. Because of the differences between the parameters in our calculation and Ref. 31, however, we should also consider the difference in the basis describing the states of the four-atom cluster. Although the fully polarized local moment ground state has been assumed for ferromagnetic bcc Fe in Ref. 31, the basis is specified by the occupancy of each spin state at each site in our calculation. Hence, our calculation takes into consideration the majority-spin hole existing in the valence band of Fe. This difference in the cluster basis may also cause the differ-

ences between parameters in our calculation and Ref. 31.

The parameters obtained for the two films are analogous, which indicates that the electronic states of the Fe thin films in regions I and II are similar near the surface. In Fig. 4(b), however, the intensity near the peak in the calculated majority-spin spectrum for 6.6 ML Fe is displaced to slightly higher binding energy than the experimental spectrum. This difference is attributed to the spectral weight in the experimental majority-spin spectrum located at the peak position of the minority-spin spectrum. Since in materials with no ferromagnetic order the majority- and minority-spin spectra show no difference, the above feature in the experimental SRPES spectrum for 6.6 ML Fe can be explained by the overlap with the signal from deeper layers, in which the averaged magnetic moment is suppressed. If the SRPES spectrum of 6.6 ML Fe is compared to that of 3.9 ML Fe in detail, one finds that the intensity at about 95 eV is still weaker in the majority-spin spectrum of 6.6 ML Fe. The small differences between the parameters of 6.6 and 3.9 ML Fe in Table I result from this slight difference in the spectral shape.

IV. CONCLUSION

We have studied the magnetism of fcc Fe thin film on Co(100) and its thickness dependence by Fe 3*s* SRPES. The characteristics of the Fe 3*s* SRPES spectra for fcc Fe thin films have been also investigated by analyzing them by the cluster model calculation consisting of four Fe atoms. The Fe 3*s* SRPES spectra were measured on 3.9 and 6.6 ML Fe thin films, as representatives of the region I and II films, respectively. The spin polarizations of Fe 3*s* SRPES spectra for 3.9 and 6.6 ML Fe indicate that the magnetic moments in regions I and II are equivalent near the surface, whereas the magnetic moment averaged up to deeper layers of the Fe thin film is suppressed in region II. The cluster model calculation shows that both of the Fe thin films in regions I and II are in the high-spin ferromagnetic state near the surface. The Fe 3*s* majority-spin spectra for the fcc Fe thin films exhibit weaker intensity on the high-binding-energy side of the main peak than the spectrum previously reported for bcc Fe. The cluster model calculation shows that the features observed in the Fe 3*s* SRPES spectra are attributed mainly to the larger t in the fcc Fe thin films than in bcc Fe owing to the structural characteristic. The roles of the interatomic configuration interaction are elucidated in the 3*s* SRPES spectra for fcc Fe thin films on Co(100) by the cluster model calculation.

ACKNOWLEDGMENT

We would like to thank A. Harasawa and K. Hayashi for their technical support in the experiments.

[1] V. L. Moruzzi and P. M. Marcus, in *Handbook of Magnetic Materials*, edited by K. H. J. Buschow (Elsevier, Amsterdam, 1993), Vol. 7, p. 97.
[2] M. Wuttig and X. Liu, *Ultrathin Metal Films* (Springer, Berlin, 2004).
[3] O. Rader, T. Mizokawa, A. Fujimori, and A. Kimura, Phys. Rev. B **64**, 165414 (2001).
[4] M. Sawada, K. Hayashi, and A. Kakizaki, Phys. Rev. B **63**, 195407 (2001).
[5] V. L. Moruzzi, P. M. Marcus, and J. Kübler, Phys. Rev. B **39**, 6957 (1989).
[6] M. Uhl, L. M. Sandratskii, and J. Kübler, Phys. Rev. B **50**, 291 (1994).
[7] Y. Zhou, W. Zhang, L. Zhong, X. Nie, and D.-S. Wang, J. Magn. Magn. Mater. **167**, 136 (1997).
[8] D. Pescia, M. Stampanoni, G. L. Bona, A. Vaterlaus, R. F. Willis, and F. Meier, Phys. Rev. Lett. **58**, 2126 (1987).
[9] J. Thomassen, F. May, B. Feldmann, M. Wuttig, and H. Ibach, Phys. Rev. Lett. **69**, 3831 (1992).
[10] D. Li, M. Freitag, J. Pearson, Z. Q. Qiu, and S. D. Bader, Phys. Rev. Lett. **72**, 3112 (1994).
[11] S. Müller, P. Bayer, C. Reischl, K. Heinz, B. Feldmann, H. Zillgen, and M. Wuttig, Phys. Rev. Lett. **74**, 765 (1995).
[12] M. Wuttig, B. Feldmann, and T. Flores, Surf. Sci. **331-333**, 659 (1995).
[13] V. Popescu, H. Ebert, L. Szunyogh, P. Weinberger, and M. Donath, Phys. Rev. B **61**, 15 241 (2000).
[14] A. Biedermann, R. Tscheließnig, M. Schmid, and P. Varga, Phys. Rev. Lett. **87**, 086103 (2001).
[15] T. Bernhard, M. Baron, M. Gruyters, and H. Winter, Phys. Rev. Lett. **95**, 087601 (2005).
[16] U. Gradmann and H. O. Isbert, J. Magn. Magn. Mater. **15-18**, 1109 (1980).
[17] W. L. O'Brien and B. P. Tonner, Surf. Sci. **334**, 10 (1995).
[18] E. J. Escorcia-Aparicio, R. K. Kawakami, and Z. Q. Qiu, Phys. Rev. B **54**, 4155 (1996).
[19] N. Kamakura, A. Kimura, O. Rader, A. Harasawa, and A. Kakizaki, J. Electron Spectrosc. Relat. Phenom. **92**, 45 (1998); N. Kamakura, A. Kimura, K. Hayashi, A. Harasawa, and A. Kakizaki, Jpn. J. Appl. Phys., Suppl. **38-1**, 415 (1999).
[20] R. Kläsges, D. Schmitz, C. Carbone, W. Eberhardt, and T. Kachel, Solid State Commun. **107**, 13 (1998).
[21] X. Gao, M. Salvietti, W. Kuch, C. M. Schneider, and J. Kirschner, Phys. Rev. B **58**, 15 426 (1998).
[22] D. Schmitz, C. Charton, A. Scholl, C. Carbone, and W. Eberhardt, Phys. Rev. B **59**, 4327 (1999).
[23] A. Dallmeyer, K. Maiti, O. Rader, L. Pasquali, C. Carbone, and W. Eberhardt, Phys. Rev. B **63**, 104413 (2001).
[24] K. Hayashi, M. Sawada, A. Harasawa, A. Kimura, and A. Kakizaki, Phys. Rev. B **64**, 054417 (2001); K. Hayashi, M. Sawada, H. Yamagami, A. Kimura, and A. Kakizaki, J. Phys. Soc. Jpn. **73**, 2550 (2004).
[25] J. H. Van Vleck, Phys. Rev. **45**, 405 (1934).
[26] P. S. Bagus, A. J. Freeman, and F. Sasaki, Phys. Rev. Lett. **30**, 850 (1973).
[27] J. F. van Acker, Z. M. Stadnik, J. C. Fuggle, H. J. W. M. Hoekstra, K. H. J. Buschow, and G. Stroink, Phys. Rev. B **37**, 6827 (1988).

[28] S.-J. Oh, G.-H. Gweon, and J.-G. Park, Phys. Rev. Lett. **68**, 2850 (1992).
[29] K. Okada and A. Kotani, J. Phys. Soc. Jpn. **61**, 4619 (1992).
[30] P. Krüger, M. Taguchi, J. C. Parlebas, and A. Kotani, Phys. Rev. B **55**, 16 466 (1997).
[31] K.-H. Park, S.-J. Oh, K. Shimada, A. Kamata, K. Ono, A. Kakizaki, and T. Ishii, Phys. Rev. B **53**, 5633 (1996).
[32] F. U. Hillebrecht, R. Jungblut, and E. Kisker, Phys. Rev. Lett. **65**, 2450 (1990).
[33] C. Carbone, T. Kachel, R. Rochow, and W. Gudat, Solid State Commun. **77**, 619 (1991).
[34] T. Kachel, C. Carbone, and W. Gudat, Phys. Rev. B **47**, 15 391 (1993).
[35] Z. Xu, Y. Liu, P. D. Johnson, B. Itchkawitz, K. Randall, J. Feldhaus, and A. Bradshaw, Phys. Rev. B **51**, 7912 (1995).
[36] P. D. Johnson, Y. Liu, Z. Xu, and D.-J. Huang, J. Electron Spectrosc. Relat. Phenom. **75**, 245 (1995).
[37] W. J. Lademan and L. E. Klebanoff, Phys. Rev. B **54**, 11 725 (1996).
[38] S. Shin, Y. Tezuka, T. Kinoshita, A. Kakizaki, T. Ishii, Y. Ueda, W. Jang, H. Takei, Y. Chiba, and M. Ishigame, Phys. Rev. B **46**, 9224 (1992).
[39] E. U. Condon and G. H. Shortley, *The Theory of Atomic Spectra* (Cambridge University Press, Cambridge, U.K., 1935).
[40] A. Kakizaki, H. Ohkuma, T. Kinoshita, A. Harasawa, and T. Ishii, Rev. Sci. Instrum. **63**, 367 (1992).
[41] J. Fujii, T. Kinoshita, K. Shimada, T. Ikoma, A. Kakizaki, T. Ishii, H. Fukutani, A. Fujimori, K. Soda, and H. Sugawara, in *Proceedings of the International Symposium on High Energy Spin Physics*, edited by T. Hasegawa, N. Horikawa, A. Masaike, and S. Sawada (Universal Academy Press, Tokyo, 1992), p. 885.
[42] E. Dagotto and A. Moreo, Phys. Rev. D **31**, 865 (1985); E. Dagotto, R. Joynt, A. Moreo, S. Bacci, and E. Gagliano, Phys. Rev. B **41**, 9049 (1990).
[43] R. Haydock, V. Heine, and M. J. Kelly, J. Phys. C **5**, 2845 (1972); **8**, 2591 (1975).
[44] O. Heckmann, H. Magnan, P. le Fevre, D. Chandesris, and J. J. Rehr, Surf. Sci. **312**, 62 (1994).
[45] For an estimation of the expanded layer distance, we refer to the similar system Fe/Cu(100). The similarity is also understood from the lattice parameter of substrate Cu(100) which is equal to that of fcc Co(100) thin film (3.61 Å) on Cu(100). In Fe/Cu(100), the layer distance is expanded to ~1.87 Å at the whole Fe thin film in region I and the two topmost layers in region II (Refs. 2 and 12). From the layer distance of ~1.87 Å, the distance to the distorted eight sites in the fct Fe layers is estimated to be ~2.60 Å.